A dynamic representation of target motion drives predictive smooth pursuit during target blanking

Jean-Jacques Orban de Xivry
CESAME, Université catholique de Louvain, Louvain-La-Neuve, Belgium, & Laboratory of Neurophysiology, Université catholique de Louvain, Brussels, Belgium

Marcus Missal
CESAME, Université catholique de Louvain, Louvain-La-Neuve, Belgium, & Laboratory of Neurophysiology, Université catholique de Louvain, Brussels, Belgium

Philippe Lefèvre
CESAME, Université catholique de Louvain, Louvain-La-Neuve, Belgium, & Laboratory of Neurophysiology, Université catholique de Louvain, Brussels, Belgium

Moving objects are often occluded by neighboring objects. In order for the eye to smoothly pursue a moving object that is transiently occluded, a prediction of its trajectory is necessary. For targets moving on a linear path, predictive eye velocity can be regulated on the basis of target motion before and after the occlusions. However, objects in a more dynamic environment move along more complex trajectories. In this condition, a dynamic internal representation of target motion is required. Yet, the nature of such an internal representation has never been investigated. Similarly, the impact of predictive saccades on the predictive smooth pursuit response has never been considered. Therefore, we investigated the predictive smooth pursuit and saccadic responses during the occlusion of a target moving along a circular path. We found that the predictive smooth pursuit was driven by an internal representation of target motion that evolved with time. In addition, we demonstrated that in two dimensions, the predictive smooth pursuit system does influence the amplitude of predictive saccades but not vice versa. In conclusion, in the absence of retinal inputs, the smooth pursuit system is driven by the output of a short-term velocity memory that contains the dynamic representation of target motion.

Keywords: eye movements, prediction, saccade pursuit interaction, occlusion, smooth pursuit

Citation: Orban de Xivry, J.-J., Missal, M., & Lefèvre, P. (2008). A dynamic representation of target motion drives predictive smooth pursuit during target blanking. *Journal of Vision, 8*(15):6, 1–13, http://journalofvision.org/8/15/6/, doi:10.1167/8.15.6.

Introduction

Prediction is a feature inherent to various motor systems. In particular, prediction allows the oculomotor system to track a target moving along a predictable path in synchrony by overcoming the inherent time delays present in the visual system (Bahill & McDonald, 1983; Barnes & Asselman, 1991; Barnes, Barnes, & Chakraborti, 2000; Dallos & Jones, 1963).

The predictive mechanisms driving the smooth pursuit response during the temporary occlusion of a moving target have been widely studied in one dimension (Becker & Fuchs, 1985; Mitrani & Dimitrov, 1978). In this case, both position (Barborica & Ferrera, 2004; Filion, Washburn, & Gulledge, 1996) and velocity (Barborica & Ferrera, 2003; Ilg & Thier, 2003) of the occluded target can be predicted by the oculomotor system. However, around 100 ms after target disappearance, the eye velocity starts to decay exponentially. Either it continues decreasing until zero when the target is not expected to reappear or it reaches a plateau value when it is expected to reappear (Becker & Fuchs, 1985; de Brouwer, Missal, & Lefèvre, 2001; Mitrani & Dimitrov, 1978; Pola & Wyatt, 1997). Eye velocity decay might be due to either a reduction in the gain that regulates smooth pursuit eye movements (Churchland & Lisberger, 2002; Tanaka & Lisberger, 2001) or to a reduction of target motion signals held in short-term memory. In contrast, when the duration of the occlusion is known in advance, predictive eye velocity recovery takes place before the end of the occlusion period (Bennett & Barnes, 2003, 2004, 2005). In addition, the level of this

doi: 10.1167/8.15.6 Received April 16, 2008; published November 17, 2008 ISSN 1534-7362

recovery is scaled to the expected target velocity at the moment of target reappearance (Bennett & Barnes, 2004, 2006b; Orban de Xivry, Bennett, Lefèvre, & Barnes, 2006). Importantly, this predictive eye velocity recovery demonstrated that the predictive pursuit observed during the periods of occlusion was influenced by post-occlusion target velocity information. Therefore, providing information about post-occlusion target position and/or velocity influences the oculomotor response during blanking (Mrotek & Soechting, 2007; Orban de Xivry et al., 2006). Similarly, predictive pursuit is also influenced by pre-occlusion target velocity information. Indeed, the pre-occlusion target velocity determines the plateau value to which eye velocity decays (Becker & Fuchs, 1985). In sum, both pre- and post-occlusion information could influence the oculomotor behavior during target blanking. Thus, it is important to minimize the influence of pre- and post-occlusion information when studying the nature of the internal representation of target velocity driving the predictive oculomotor response during periods of occlusion. This can be achieved by combining non-uniform target motion (i.e., not uniform rectilinear target motion) with randomized durations of occlusion.

Uniformly accelerated motion, a type of non-uniform target motion, has been used to investigate the representation of target motion and to minimize the influence of pre-occlusion information (Bennett & Barnes, 2006b; Bennett, Orban de Xivry, Barnes, & Lefèvre, 2007). However, in these studies, the duration of the occlusions was constant and post-occlusion information drives predictive pursuit. Predictive pursuit of an invisible sinusoidally moving target, another type of non-uniform target motion, has also been tested. For instance, Barnes et al. (2000) found that, when the sinusoidally moving target disappeared after half a cycle (i.e., at target reversal), subjects were able to increase their eye velocity for a period of 200 ms after which it decayed to zero. However, it was not clear whether the observed pursuit response was part of an active tracking of the invisible target or corresponded to the end of the pursuit response after the sudden disappearance of the tracked target (OFF-response: Pola & Wyatt, 1997). In the same vein, Whittaker and Eaholtz (1982) observed that subjects were able to track a sinusoidally moving target for almost 1 s.

The present study addresses the nature of the dynamic internal representation of target motion that allows subjects to track an invisible target moving along a circular path for several hundred milliseconds. To do so, we investigated the predictive smooth pursuit response during the occlusion of a pursued target. To minimize the influence of pre- and post-occlusion target velocity information on the predictive pursuit, we made the target moving along a circular path and we randomized the duration of the blanking periods. The predictions of models integrating either a static or a dynamic internal representation of target velocity were compared with the actual predictive smooth pursuit response. The results of this comparison demonstrate that a dynamic internal representation of future target motion drives the predictive smooth pursuit response during occlusions. Furthermore, this effect is independent of the position of the eyes with respect to the occluded target. We suggest that this dynamic internal representation of target motion influences the tracking of both visible and invisible predictable targets.

Methods

Subjects

Six human subjects participated in the experiment after informed consent. Their ages ranged between 22 and 40 years. Four of them were completely naive to the purposes of the experiment. They all had normal or corrected-to-normal vision and did not have any known oculomotor abnormality. All procedures were approved by the Université catholique de Louvain ethics committee and were in agreement with the Declaration of Helsinki.

Paradigm

Subjects were asked to pursue a visual target following a counterclockwise circular path (see Figure 1). After a period of fixation of 500 ms, the target began to move and remained visible for at least a half-circle (3.3 to 4 s). Subsequently, there were three successive periods of target occlusion (represented by gray bars in Figure 1C) ranging from 400 to 1000 ms. After each of the three occlusions, the target reappeared for a period ranging between 800 ms and 1500 ms. Thus, each test trial consisted of four periods of visible target interleaved with three periods of occlusion. At the end of each trial, the target was switched off for 2 s.

The characteristics of the circular path varied randomly across trials. Both radius (9.6, 12.8, and 16 deg) and frequency (0.15, 0.2, and 0.25 Hz) were varied. The combination of the different radii and frequencies led to 5 different vectorial target velocities ranging from 9 to 25 deg/s (the vectorial velocity is the modulus of the velocity vector). The starting point of the circular trajectory (θ_0) was chosen at random on the circular path for each trial.

Experimental sessions consisted of several blocks of 13 test trials and lasted a maximum of 30 minutes. Each subject performed at least four experimental sessions, which led to a minimum of 810 periods of occlusion per subject (maximum: 1125). At the beginning of each session, a learning block was presented to the subjects. It consisted of 13 learning trials during which the visual target moved counterclockwise on a circular path with the same parameters (radius and frequency) used in the test trials. However, the target was never switched off and

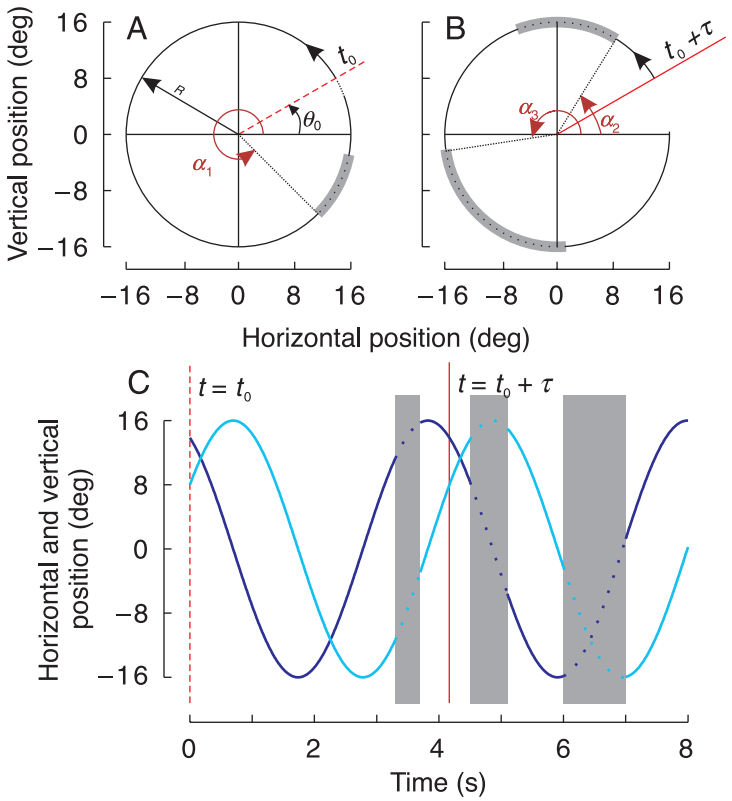

Figure 1. Representation of target motion in XY plots (panels A and B) and in position vs. time plot (panel C). In the XY plots, panel A represents the first revolution of the target along the circular path of radius, R. At time t_0, the target appeared at (R, θ_0) in polar coordinates (represented by the dashed red line) and began to move counterclockwise along the circular path. The second revolution of the target is represented in panel B. It began at time $t_0 - \tau$, where τ is the period of target motion (represented by the continuous red line). During the revolutions, the target was occluded three times (dotted black lines on gray thick lines). The starting angles of the occlusions are given by α_1, α_2, and α_3. In panel C, we represented the horizontal (dark blue) and vertical (light blue) target positions vs. time for the same two revolutions as in previous panels. Dotted lines on gray bars represented the occlusion periods. Time correspondence between panels A, B, and C is provided by the dashed and solid red lines that delimit the starting time of each of the two revolutions.

remained visible for the whole duration of the learning trials (5 s).

Experimental setup and data analysis

Subjects sat in complete darkness in front of a translucent screen, which was at a distance of 1 meter and covered a field of ±40 deg horizontally and vertically. The target (0.2 deg) was a red laser spot, which was back-projected onto the screen by two mirror galvanometers. The galvanometers were controlled by a dedicated real-time computer, which controlled their position and illumination (see a detailed description of the setup in Blohm, Missal, & Lefèvre, 2003). Eye movements were recorded using the scleral coil technique (Collewijn, van der Mark, & Jansen, 1975; Robinson, 1963).

Eye and target positions were sampled at 500 Hz and stored on a hard disk for off-line analysis, which was performed using Matlab (Mathworks, Natick, MA, USA). Position signals were low-pass filtered using a zero-phase digital filter (an autoregressive, forward and backward filter, with a cutoff frequency of 48 Hz). Velocity and acceleration signals were derived from eye position by means of a central difference algorithm. All the trials were visually inspected and abnormal trials (blinks) were eliminated from the database. In addition, we removed all occlusions from the data that were interpreted by the subjects as the end of the trial (outlier analysis based on three standard deviations from the mean, which led to the rejection of 2.5% of the trials).

Saccades were detected using an acceleration threshold of 500 deg/s^2 and were labeled predictive if their onset occurred at least 170 ms after the start of the occlusion period. The first visually guided saccades after the end of the occlusion period were selected if their onset occurred within a time interval ranging from 75 to 400 ms after the end of the occlusion. Measures of position error or heading direction were taken 25 ms before and after each saccade. To evaluate the smooth pursuit response, we analyzed both the vectorial eye velocity profile and the pursuit heading direction. The vectorial velocity corresponds to the square root of the sum of the squared horizontal and vertical components. The heading direction

of the smooth pursuit response was computed as the direction of the tangent to the smooth eye position trace. The time courses for the eye and the target heading direction during the occlusion periods were measured relative to the heading of the target at the start of the occlusion. Finally, it is worth mentioning that the vectorial eye velocity (V) is a good approximation of the angular eye velocity (ω) as $V = R * \omega$. Since R remains approximately constant during the occlusions (vectorial eye position is equal to or larger than 95% of the radius of the circular trajectory 400 ms after the start of the occlusion and at its end), the angular eye velocity is directly proportional to the vectorial eye velocity.

Moreover, the horizontal and vertical eye velocity profiles (EV) were fitted with a non-linear function resulting from the multiplication of the target velocity (TV) by a negative exponential (Figure 2). For the static memory model, TV was constant and equal to the corresponding component of the target velocity at target disappearance. For the dynamic memory model, TV varied and was equal to the actual target velocity at a specific instant in time. The parameters of the fit were the following: g, the eye velocity gain at the start of the occlusion; T, the time at the start of the eye velocity decay; G, the value of the eye velocity gain after the exponential decay; and τ, the time constant of the negative exponential. The constants were the following: R, the radius of the circular path; ω, the angular velocity of the target; and ϕ, the angular target phase at the start of the occlusion. The non-linear regression was performed on the average velocity profiles using a least-square approximation (lsqcurvefit in Matlab). The same non-linear functions were used to fit vectorial eye velocity profiles.

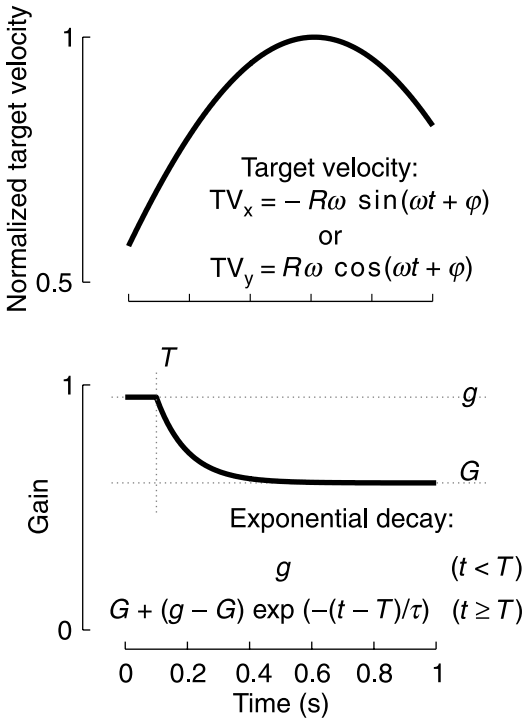

Figure 2. Illustration of the non-linear function used to characterize the eye velocity profile during occlusions. This function resulted from the multiplication of the target velocity (upper panel) with a negative exponential (lower panel). The parameters of the non-linear function that were fitted on the data were the following: g, the gain at the start of the occlusion; G, the plateau value; T, the time at the start of the eye velocity decay; and τ, the time constant of the exponential. The constants were the following: R, the radius of the circle; ω, the target angular velocity; and ϕ, the angular position of the target at the start of the occlusion period.

Statistical analyses (ANOVA, T-test) were performed using Statistica (Statsoft, Tulsa, OK, USA). Sample means were compared using T-tests. To account for multiple comparisons, the p-values were corrected by means of the false discovery rate procedure (Curran-Everett, 2000).

Finally, throughout the analyses, some variables were expressed in polar coordinates (such as the angular target velocity). The angular component of the polar coordinates was expressed in degrees, noted deg_p. This is in contrast to the degree unit of visual angle, noted deg. The three frequencies (0.15, 0.2, and 0.25 Hz) of the target led to angular velocities of 54, 72, and 90 deg_p/s, respectively.

Results

Figure 3 shows a typical example of the oculomotor response during the occlusion of a target moving along a circular path. The occlusion of the pursuit target was associated with decays in the vectorial and angular smooth eye velocities that were often accompanied by the release of one or more predictive saccades (Figure 3, saccades #1 and #2). However, the vectorial eye velocity did not decay to zero but instead reached a plateau value. The pattern of this response (decay in vectorial eye velocity and predictive saccades) was typical and occurred in about 90% of the occlusions. In addition, more than 75% of the occlusions were accompanied by at least one saccade (75% to 91% across subjects, except for subject #6 with 19%). Therefore, the data from subject #6 were not included for analyses related to saccades. Typically, a visually guided catch-up saccade corrected for the position error at the end of the occlusion (Figure 3, saccade #3).

There was a general tendency for the first saccades in the occlusion to be centripetal, which means that they brought the eye toward the center of the circle. In contrast, the second saccades were generally parallel to the circular path of the target (Figure 3A). Both the first and second saccades gave a phase advance to the eye with respect to the target. This feature appears clearly in Figure 3 by means of the isochronic lines, connecting the eye and target at the same instant in time (thin black lines in

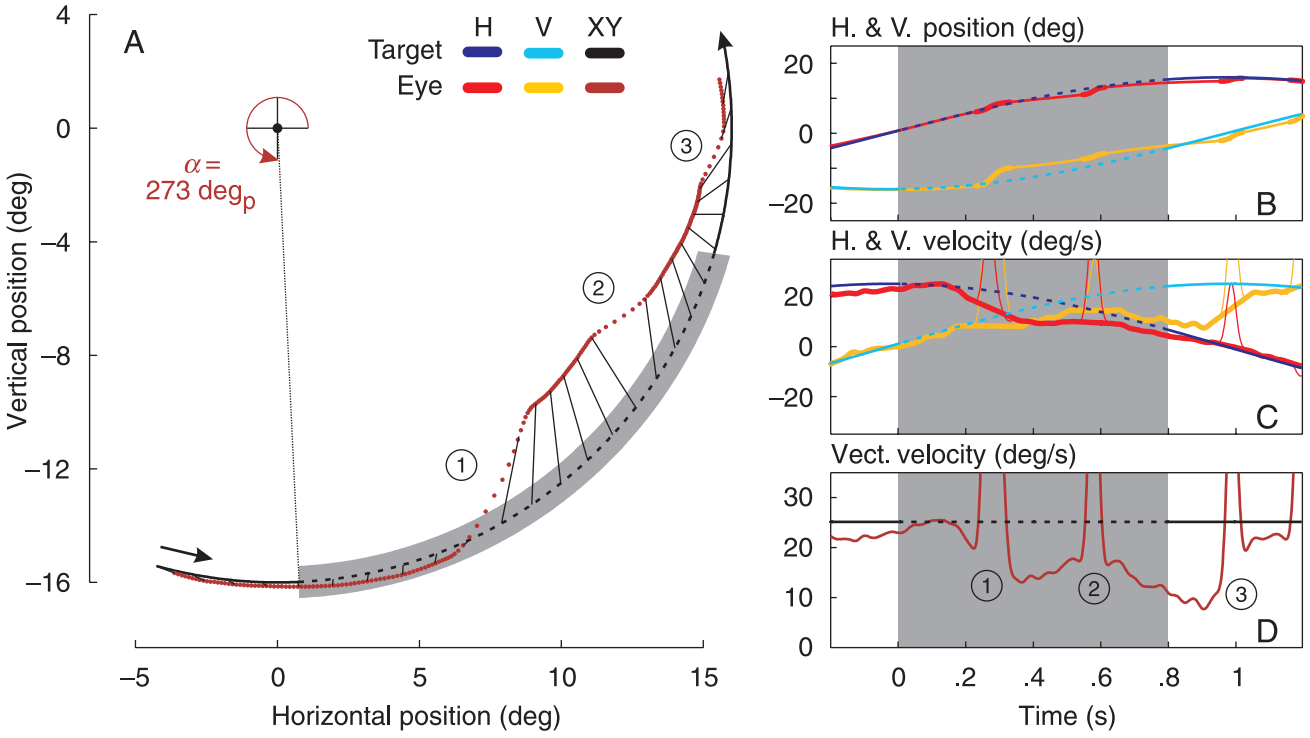

Figure 3. Typical oculomotor response during occlusions. The color code for the four panels is given on top of panel A (H: horizontal; V: Vertical; XY: 2D or vectorial). Panel A is the XY plot of both the eye and target from 200 ms before the occlusion until 400 ms after the occlusion. The origin of the reference frame coincides with the center of the circular path and the occlusion had a starting angle of 273 deg_p. The brown trace represents eye position sampled every 6 ms. Saccades are labeled 1, 2, and 3, and are represented by dotted epochs on the brown trace. Panels B, C, and D represent position, velocity, and vectorial velocity vs. time, respectively, for both the eye and target. In panel B, the saccades are represented by a thicker trace. In panel C, the desaccaded smooth eye velocity is given by the thicker trace. The occlusion interval is delimited by the gray area. Target velocity was 25 deg/s.

Figure 3A). Indeed, before the saccades, the eye lagged behind the target whereas it was ahead of the target afterward. Isochronic lines also show that at the end of the occlusion period, the eye and target were in phase for this particular example (Figure 3). This phase synchronization between the eye and the target resulted from the combination of saccadic and smooth pursuit predictive eye movements.

Smooth response

As illustrated by the typical example, smooth eye velocity tended to decay during the occlusions (Figure 3D). In agreement with previous studies in one dimension, we found that the vectorial eye velocity exponentially decayed after the target disappearance (Figure 4A). The time constant of the exponential function ranged from 0.07 to 0.13 s depending on the subject, except for subject #6 who had a very modest decay associated with a time constant of 0.033 s. This decay in the smooth response usually did not last for the whole occlusion. After a few hundred milliseconds, the vectorial eye velocity reached a plateau, the gain of which varied across subjects (from 0.54 to 0.85) and across target velocities (ANOVA, $p < 0.001$). Surprisingly, this gain did not depend on the duration of the occlusion period for four of the six subjects (ANOVA, $p > 0.05$ in at least 7 out of the 9 target conditions). The last two subjects showed a significant decrease in their gain relative to occlusion duration in the majority of the target conditions (7 and 8 of the 9 conditions). In addition, for all subjects, the gain was independent of the number of occlusion (first, second, or third occlusion within the trial, Tukey Post-Hoc tests, $p > 0.05$). This demonstrates that half a revolution was sufficient in our paradigm to build an accurate dynamic representation of target motion.

In two dimensions, the vectorial eye velocity is not sufficient to characterize the smooth pursuit response. The heading direction (namely, the orientation) of the pursuit response must also be taken into consideration. Thus, the heading direction was computed relative to the target heading direction at the target offset (see Methods). During the course of the occlusion period, the heading direction of the target evolved over time (solid trace in Figure 4B). Interestingly, the oculomotor system was able to accurately predict the heading of the target (dashed trace in Figure 4B). Indeed, the pursuit heading direction matched the target heading direction almost perfectly during the first 600 ms of the occlusions.

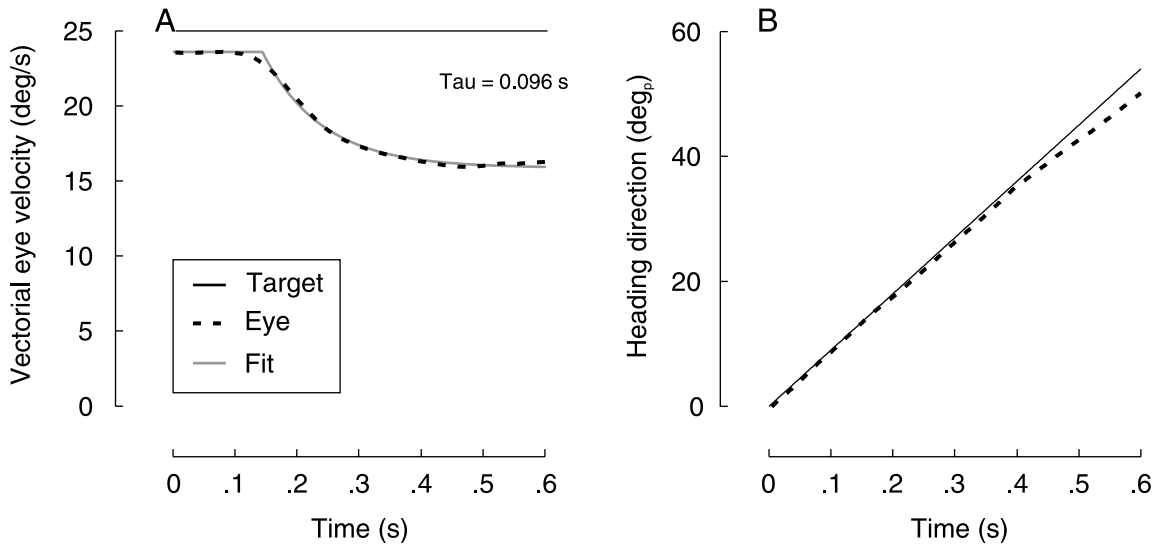

Figure 4. Average smooth pursuit response during the first 600 ms of the occlusions. Panel A is the average of vectorial velocity vs. time for both the eye (dashed line) and target (solid line). A negative exponential was fitted on the eye trace (dark gray curve, see Methods). Standard error of the mean was smaller than 1 deg/s. Panel B is the average of the heading directions for both the eye (dashed black curve) and target (black line). All the heading directions were computed with respect to the heading direction of the target at the start of the occlusion. Standard error was smaller than 1 deg_p and was therefore not represented. Occlusions from all subjects lasting more than 600 ms were selected and averaged for these graphs. Target velocity was 25 deg/s.

In order to assess what drove the predictive smooth pursuit response during occlusions, we compared the predictions made by two different models. One model incorporated a static memory, and the other model incorporated a dynamic one (see Methods). During occlusions, the static memory contained information about pre- and post-occlusion target motion but no information related to target motion during the period of occlusion. Since the duration of the occlusions was unpredictable and target velocity was non-uniform (i.e., not uniform rectilinear), post-occlusion information was not available. Therefore, the static model represents the hypothesized smooth pursuit response if it was based only on pre-occlusion information. In sum, the static memory contained a constant value for the target velocity whereas the dynamic memory held a representation of the target velocity that evolved with time. For instance, when considering the group of occlusions starting a few hundred milliseconds before the target crossed the horizontal or vertical axis (groups A and B in Figure 5), the static and dynamic models made different predictions regarding the predictive smooth pursuit response. In order to illustrate these predictions, we focused on the horizontal (resp. vertical) components of the eye and target velocities for the occlusions contained in group A (resp. B). We focused on the horizontal components because the sign of the horizontal (resp. vertical) target velocity changed during these occlusions (target velocity is represented by the colored solid traces labeled "T" in Figure 5A, resp. Figure 5B). The static memory model predicted that the studied component of the smooth eye velocity should exponentially decay with respect to the target velocity during occlusions (colored dashed traces labeled "S" in Figures 5A and 5B). Thus, this component of smooth eye velocity should reach a plateau value after a few hundred milliseconds. In contrast, the dynamic memory model suggested that this component of the eye velocity should be close to the corresponding component of the target velocity held in the dynamic memory. However, these components should not match because of the exponential decay present in the dynamic memory model (white dashed lines labeled "D" in Figures 5A and 5B). Therefore, this model predicts that the component of smooth eye velocity should increase during occlusions but at a lower rate than the target velocity.

Other predictions made by the two models are illustrated in Figures 5C and 5D. In these cases, we focused on the occlusions starting just after the target crossed either the horizontal or vertical axis (groups C and D in Figure 5). For these groups of occlusions, one component of the target velocity increased continuously during the first 600 ms of the occlusions (colored solid traces in Figures 5C and 5D). In this case, the static model predicts that the predictive smooth eye velocity should first increase and subsequently decrease exponentially during occlusions (colored dashed traces labeled "S" in Figures 5C and 5D). In contrast, the dynamic model predicts that the smooth eye velocity should increase during occlusions (white dashed traces labeled "D" in Figures 5C and 5D).

In each analysis, our data unambiguously supported the dynamic memory model. Indeed, the predictions of this model lie within the confidence interval of the mean eye velocity profiles (colored area around the white dashed traces in Figure 5), yielding a remarkably good fit between

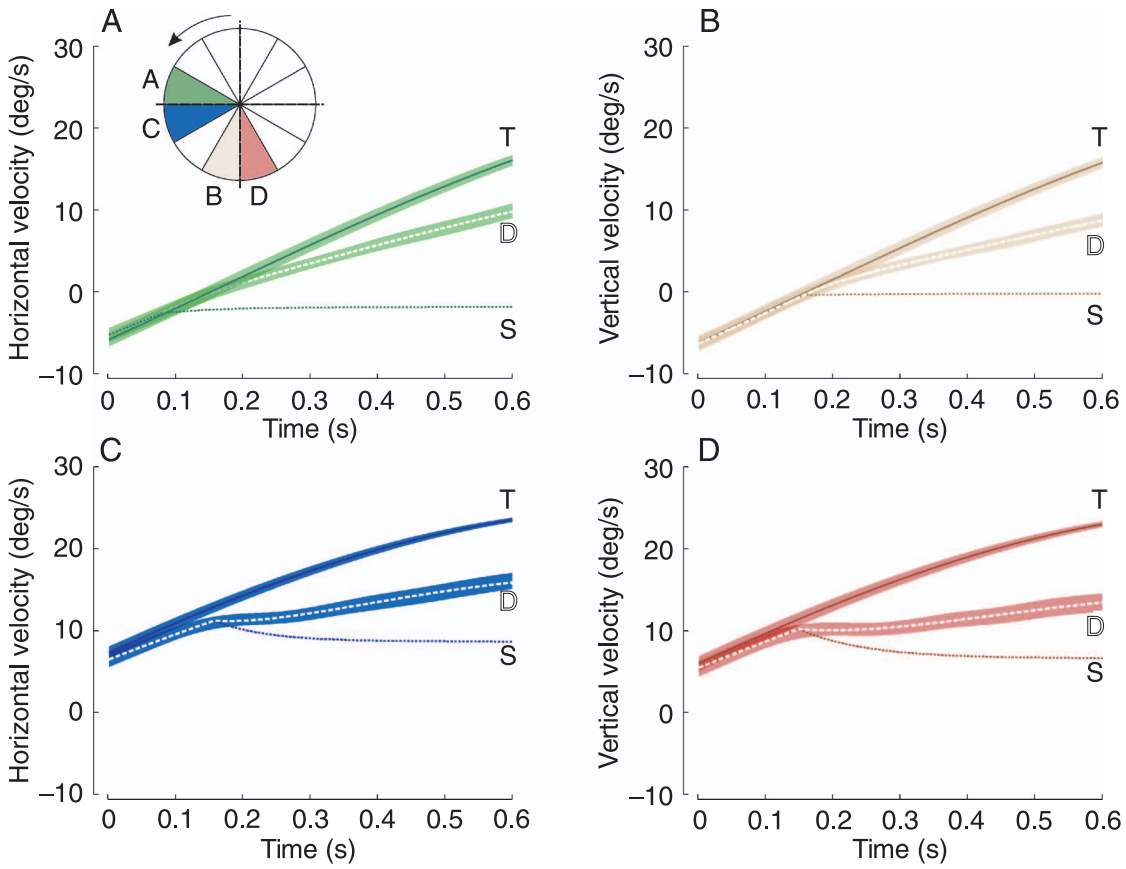

Figure 5. Mean horizontal and vertical velocity components for different groups of occlusions. Panels A, B, C, and D are the horizontal and vertical components of target velocity (solid colored traces) vs. time for different groups of trials (reference to panels A–B–C–D). The horizontal velocity is shown for panels A and C. The vertical velocity is shown for panels B and D. The confidence interval of the mean eye velocity traces is represented by the colored area (means not shown). The fit of the static memory model is represented by thin dotted lines (label "S"). The fit of the dynamic memory model is represented by white dashed traces (label "D", see Methods). Inset: Categorization of the occlusions regarding their starting angle (see Figure 1) by bins of 30 deg_p. Groups I and III (resp. II and IV) contain the occlusions starting just before (resp. after) the crossing of the horizontal or vertical axis, i.e., group I contains the occlusions with a starting angle between 150 and 180 deg_p and between 330 and 0 deg_p (with a reversed sign). A color was assigned to each group and was used in panels A–D.

the eye data observed and the dynamic model. This is in contrast with the poor predictive value of the static model. Moreover, mean fitted values (±*SE*) for the time of velocity decay (152 ± 4 ms) and for the time constant of the exponential (107 ± 8 ms) matched the values found in the literature (Becker & Fuchs, 1985). Similar results were obtained when the fits were performed for each subject separately (time of velocity decay: 153 ± 2 ms; time constant of the exponential: 126 ± 5 ms).

Pursuit heading direction matches target heading direction across saccades

The predictive smooth pursuit response during occlusions was characterized by a decrease in vectorial eye velocity but possessed a relatively accurate heading direction on average (Figure 4). This accurate heading direction supports a dynamic internal representation of target motion. However, during the occlusions, the eye trajectory was perturbed by the occurrence of predictive saccades that modified the eye position largely in a very short amount of time. The existence of a dynamic memory of target motion implies that the smooth pursuit heading should remain parallel to the target heading direction around the time of predictive saccades. To confirm the existence of a dynamic memory, we tested whether the change in smooth pursuit heading direction around the time of large predictive saccades was similar to the change in target heading direction during the same saccade. According to the hypothesis that there exists a dynamic memory of target motion, the only relevant information is the target heading direction at a given instant in time. Therefore, the pursuit heading direction should be determined by the current target heading direction independently of current eye position (Figure 6A, position independence hypothesis). Clearly, this hypothesis implies that the internal representation of target motion is dynamic, i.e., it evolves with time.

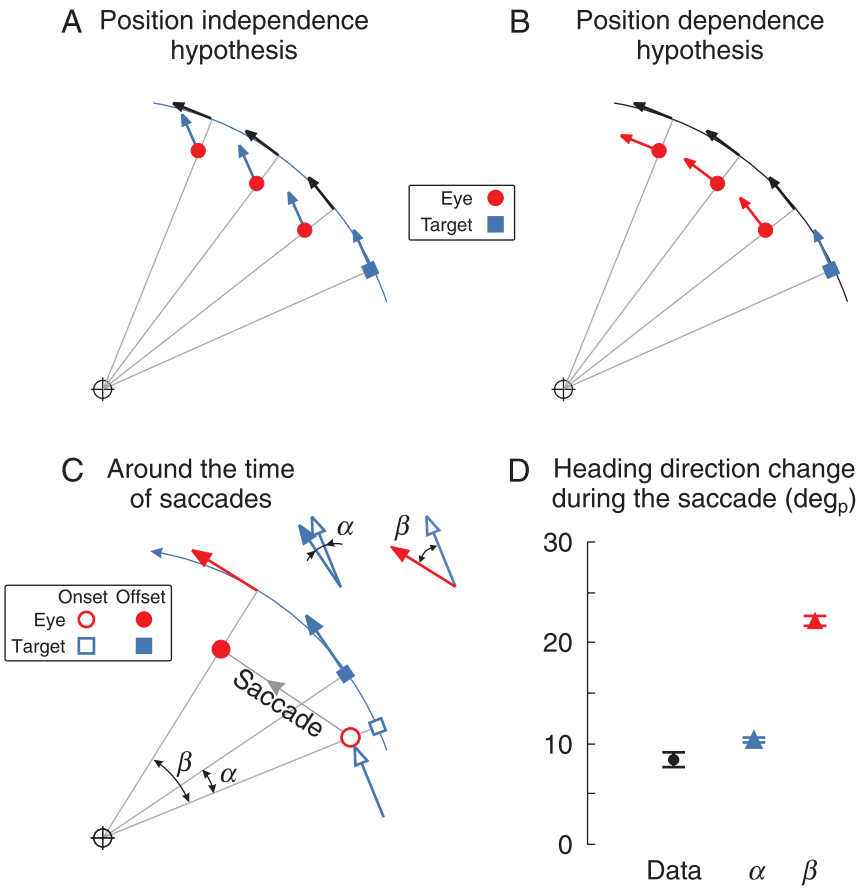

Figure 6. Hypothesized and actual change in heading direction around the time of saccades. Panels A and B are presentations of the two hypotheses. Different eye positions are represented with red disks. Target position is represented with the blue square. Heading directions for the different eye positions are represented with either red (panel A) or blue (panel B) arrows. The black arrows represent the tangent to the circular path (thin curved line) at the different angular eye positions. The center of the circle is given by the small circle. Panel A is the position dependence hypothesis, where the pursuit heading direction is parallel to the circular target path. Panel B is the position independence hypothesis, where the pursuit heading direction is parallel to the current target heading direction and independent of eye position. Panel C is an illustration of the predicted change in the heading direction during saccades following the two hypotheses. Eye (resp. target) position at saccade onset and offset is represented with red open and filled disks (resp. blue open and filled squares). α represents the predicted change following the position dependence hypothesis, whereas β gives the change predicted by the position independence hypothesis. Panel D is a comparison between the predicted and actual heading direction changes between saccade onset and offset. (All subjects and conditions pooled together.) α, prediction from the position dependence hypothesis; β, prediction from the position independence hypothesis; Data: actual eye data.

Alternatively, subjects could have followed a circular path independently of current target heading direction. In this case (Figure 6B, position dependence hypothesis), the pursuit heading direction should be determined by the angular position of the eye with respect to the circular path (Figure 6B, black arrows) and not with respect to the actual target heading direction (Figure 6B, blue square and arrow). Following this hypothesis, the only relevant information is an iconic representation of the circular path, not the actual target heading direction.

To distinguish between these two hypotheses, we tested the influence of rapid changes in eye position on pursuit heading direction around the time of the first predictive saccades (Figure 6C). As illustrated by the saccades in Figure 3, predictive saccades modified the angular position of the eye over a short time interval. During the same time interval, the change in angular target position was much smaller. Thus, if the position independence hypothesis was true (Figure 6A), changes in the pursuit heading direction should be equal to changes in the angular target position during saccades (α in Figure 6C). This prediction is due to the fact that the pursuit heading direction before and after the saccade should be parallel to the target heading direction before and after the saccade, respectively. In contrast, if the position dependence hypothesis was true, changes in the pursuit heading direction elicited by saccades should be equal to changes in the angular eye position during these saccades (β in Figure 6C). Indeed, according to the position dependence hypothesis (Figure 6B), before the saccade (resp. after the

saccade), the pursuit heading direction should be perpendicular to the radius of the circle connecting the center of the circular path to the current eye position at saccade onset (resp. at saccade offset). Therefore, according to the position dependence hypothesis, geometric rules imply that the change in pursuit heading direction should be equal to the change in angular eye position during saccades (β in Figure 6C).

In order to test these two hypotheses, we selected saccades that brought the eye at least 6 deg_p ahead of the target (30% of the first predictive saccades), yielding a significant difference between α and β. Indeed, for the selected saccades, the mean α was equal to 10.4 deg_p, whereas the mean β was equal to 22.1 deg_p (across all subjects and conditions, Figure 6D). Interestingly, the actual average change in pursuit heading direction during the saccades was equal to 8.5 deg_p (Figure 6D), which supports the position independence hypothesis, i.e., the pursuit heading direction is independent of current eye position. This hypothesis was confirmed by statistical comparisons for each of the conditions separately (3 target frequencies × 3 target radii × 5 subjects). For all conditions, the change in heading direction predicted by the position dependence hypothesis was significantly larger than the observed value (T-tests, $p < 0.05$), which was confirmed by the multiple comparison procedure. In contrast, the predictions of the heading change during the selected saccades by the position independence hypothesis were not significantly different in 35 of the 45 conditions (T-test, $p > 0.05$), when compared to the actual change. The prediction from the position independence hypothesis overestimated the actual change in the remaining 10 conditions (T-tests, $p < 0.05$). However, the significance of these 10 comparisons was rejected by the multiple comparison procedure. The same results were found when the heading was measured 50 ms after saccade offset rather than immediately at saccade offset. In sum, even around the time of predictive saccades, the pursuit heading direction was parallel to the actual target heading direction and supported a dynamic internal representation of target motion.

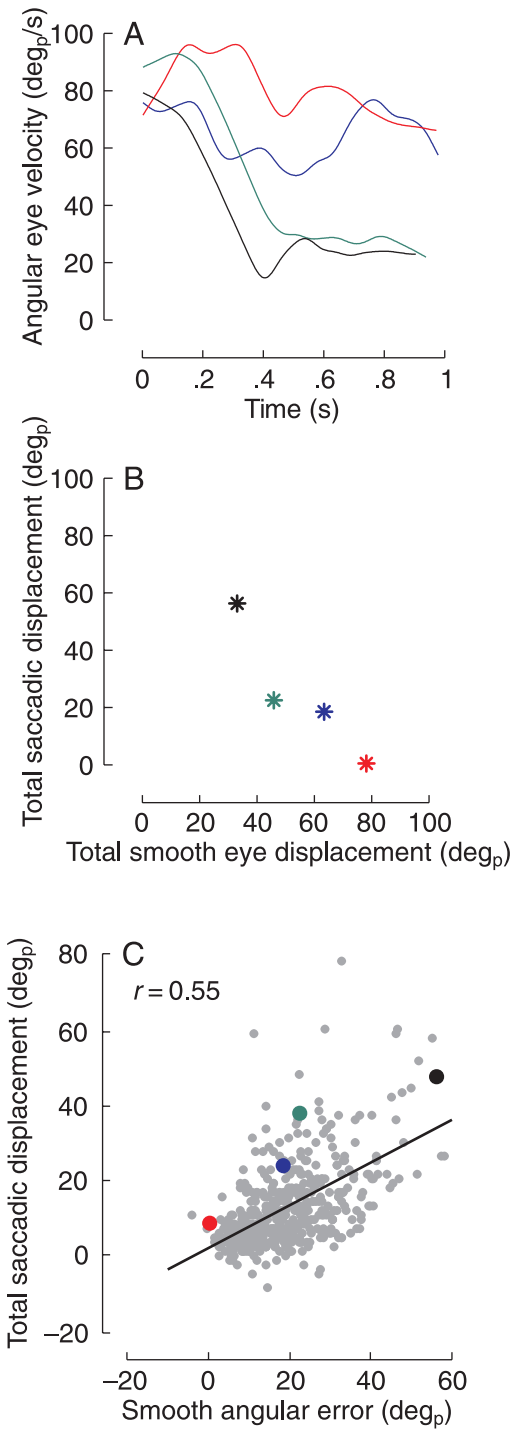

Figure 7. Saccades compensated for the variability of the predictive smooth pursuit response. Panel A is the four typical angular smooth pursuit responses during occlusions from a single subject (#2). The illustrated responses occurred during occlusions that lasted more than 0.9 s with a target velocity equal to 90 deg_p/s. These four profiles (deg_p/s) are represented vs. time (s). Panel B is the total angular saccadic displacement (sum of angular saccadic amplitudes, in deg_p) represented vs. the total smooth eye displacement (deg_p) for each of the four typical profiles represented in panel A. Panel C is the correlation between total saccadic displacement (deg_p) and smooth angular error (deg_p) for the largest target velocity. The smooth angular error corresponds to the difference between the total angular displacement of the target during the occlusion and the total angular smooth eye displacement during the same occlusion period. The four colored points correspond to the trials given in panel A. Data are pooled from all subjects.

Pursuit influences predictive saccades

During occlusions, the predictive smooth pursuit response was highly variable across occlusions (Figure 7A). For instance, although the smooth angular velocity profiles presented in Figure 7A were taken from a single subject, the angular smooth eye displacement (i.e., the

integral of the angular smooth eye velocity) achieved during these occlusions varied between 33 deg_p and 78 deg_p, for an angular target displacement of approximately 85 deg_p. Interestingly, predictive saccades compensated for the difference between the angular smooth eye displacement and the angular target displacement (i.e., the smooth angular error). Indeed, for these four trials, the sum of the angular saccadic amplitudes (i.e., the total saccadic displacement) was negatively correlated with the angular smooth eye displacement (Figure 7B). In other words, the smaller the smooth eye displacement, the larger the total saccadic displacement. This indicates that the smooth angular error was accounted for by the predictive saccades. We confirmed this result by demonstrating that for the whole population of occlusions, the total angular saccadic displacement was correlated with the smooth angular error, i.e., the difference between the angular target displacement and the angular smooth eye displacement during the occlusion (Figure 7C, $r = 0.55$, $p < 10^{-4}$, target velocity = 25 deg/s, with all subjects pooled together). This correlation was significant for each target condition when all subjects were pooled together and the correlation coefficient was between 0.21 and 0.55 (all $p < 10^{-4}$). Overall, there was significance in 34 of the 45 conditions (5 subjects × 3 frequencies × 3 radii).

Discussion

Implications for smooth pursuit models

Current models of predictive smooth pursuit response during occlusions account for exponential eye velocity decay and the predictive recovery on the sole basis of pre- and post-occlusion information (Bennett & Barnes, 2003; Churchland, Chou, & Lisberger, 2003; Madelain & Krauzlis, 2003). In these models, efference copy of pre-occlusion eye velocity or the memory of this velocity determines the plateau value to which eye velocity decays. In contrast, the predictive recovery is determined by the level of target velocity after the occlusion (Bennett & Barnes, 2006b). In our paradigm, pre-occlusion target velocity was a poor image of target velocity during the occlusion periods as target velocity was non-uniform. In addition, the post-occlusion target velocity was not available because the duration of occlusions was randomized. However, even in the absence of this information, we observed a good match between target and pursuit heading directions during the periods of blanking and specifically around the time of saccades. Therefore, we claim that the oculomotor system has access to a dynamic internal representation of target motion, i.e., a representation that evolves with time and that closely represents current target motion (Whittaker & Eaholtz, 1982).

This dynamic internal representation could either be obtained by extrapolation of the pre-occlusion target motion (Bennett et al., 2007) or assembled by the repetition of the same target motion (Bennett & Barnes, 2006a; Orban de Xivry et al., 2006). Neural correlates of this dynamic representation have been found in the frontal eye fields (FEF) where the neuronal activity reflects an up-to-date estimation of target motion during occlusions (Barborica & Ferrera, 2003, 2004; Xiao, Barborica, & Ferrera, 2007).

Such a dynamic internal representation could also come into play during visually guided smooth pursuit. Indeed, primates have the ability to track a predictable moving target with a zero-phase lag (Barnes & Asselman, 1991; Barnes et al. 2000; Barnes, Donnelly, & Eason, 1987; Barnes & Wells, 1999; Dallos & Jones, 1963), which requires prediction about future target motion. Up to now, current models have predicted target trajectory up to 100 ms in the future based on previous target motion (Bahill & McDonald, 1983; Kettner et al., 1997; Shibata, Tabata, Schaal, & Kawato, 2005). In this study, we demonstrated that humans are able to predict target motion up to 600 ms in the future. Therefore, we suggest that the dynamic internal representation that drives predictive smooth pursuit during occlusions can also drive predictive smooth pursuit during visually guided smooth pursuit.

Importance of timing information

The storage of a dynamic internal representation must be associated with an accurate estimation of the elapsed time since the start of the occlusion period. Indeed, the drive of the smooth pursuit response should be time dependent. The importance of timing information has also been emphasized in many other contexts (Buhusi & Meck, 2005; Buonomano & Karmarkar, 2002). These examples include other oculomotor studies such as the trigger for catch-up saccades during visually guided pursuit (de Brouwer, Yuksel, Blohm, Missal, & Lefèvre, 2002) and anticipation for future events (de Hemptinne, Nozaradan, Duvivier, Lefèvre, & Missal, 2007). Such timing information is also crucial in order to evoke anticipatory eye movements that occur before target motion onset (Badler & Heinen, 2006; Barnes & Asselman, 1991; Barnes & Wells, 1999; Heinen, Badler, & Ting, 2005). In our study, timing information is necessary in order to maintain the pursuit heading direction close to the target heading direction at each instant in time.

Ecological advantage

The good match between the pursuit and target heading direction during occlusions could facilitate the processing of visual motion by MT cells upon target reappearance. Indeed, attending to a particular direction of motion enhances the neuronal response to visual stimuli moving

along the attended direction (Treue & Martinez Trujillo, 1999). This enhancement changes as a function of the similarity between the attended direction and the preferred direction of the neuron (Martinez-Trujillo & Treue, 2004). In addition, some MT cells can even fire as predictors of the direction of an upcoming moving stimulus (Ferrera & Lisberger, 1997). Thus, the firing of these cells reinforces the neuronal response to stimuli in the same direction. Therefore, aligning the pursuit heading direction to the target heading direction could facilitate motion processing upon target reappearance.

Pursuit influences predictive saccades but not vice versa

A good match between the pursuit and target heading directions is not enough to optimize motion processing upon target reappearance. In addition, the projection of the target on the retina should be close to the fovea. As in many other contexts where the smooth pursuit system is limited (as reviewed in Orban de Xivry & Lefèvre, 2007), the smooth pursuit system cannot minimize position error at the moment of target reappearance independently. This is due to the exponential decay of the vectorial smooth eye velocity during occlusions. Therefore, the saccadic system compensated for the limitations of the smooth pursuit system and we observed many predictive saccades during occlusions. In agreement with a previous study (Orban de Xivry et al., 2006), these saccades compensated for the variability of the smooth pursuit response, i.e., the smaller the pursuit response, the larger the saccades. However, this relationship was one way and we showed that the predictive smooth pursuit response was not influenced by saccades during occlusions. Consequently, we hypothesize that the predictive response of the saccadic system was added to the predictive smooth pursuit response (de Brouwer, S., Missal, M., Barnes, G., & Lefèvre, 2002), without influencing it. This absence of position input for predictive smooth pursuit during occlusions is in contrast with the behavioral evidence suggesting the need of position input for the smooth pursuit system (see review in Orban de Xivry & Lefèvre, 2007). This difference between predictive and visually guided smooth pursuit responses suggests that the position input for the pursuit system should be based on sensory signals modulated by the experimental context (Blohm, Missal, & Lefèvre, 2005), not on extra-retinal signals.

Conclusion

In conclusion, the present study demonstrated that the predictive smooth pursuit response during target blanking is not solely driven by pre- and post-occlusion target motion but is driven by a dynamic internal representation of target motion during occlusions. This dynamic internal representation contains crucial timing information related to target trajectory and allows the heading of the predictive smooth pursuit to match instantaneously with the target heading during occlusions. In addition, we showed that this dynamic representation of target motion was the sole input of the smooth pursuit system. This observation was supported by the finding that the predictive smooth pursuit response did not take eye position into account. In contrast, the large variability of the predictive pursuit response was compensated for by the saccadic system. In sum, we propose that current models of predictive smooth pursuit response should be revised in order to incorporate a dynamic memory component.

Acknowledgments

This work was supported by the Fonds National de la Recherche Scientifique, the Fondation pour la Recherche Scientifique Médicale, the Belgian Program on Interuniversity Attraction Poles initiated by the Belgian Federal Science Policy Office, Actions de Recherche Concertées (French community, Belgium), an internal research grant (Fonds Spéciaux de Recherche) of the Université catholique de Louvain, and the European Space Agency (ESA) of the European Union. The scientific responsibility rests with the authors.

Commercial relationships: none.
Corresponding author: Prof. P. Lefèvre.
Email: Philippe.Lefevre@uclouvain.be.
Address: Avenue Georges Lemaitre, 4-6, B-1348 Louvain-La-Neuve, Belgium.

References

Badler, J. B., & Heinen, S. J. (2006). Anticipatory movement timing using prediction and external cues. *Journal of Neuroscience, 26,* 4519–4525. [PubMed] [Article]

Bahill, A. T., & McDonald, J. D. (1983). Smooth pursuit eye movements in response to predictable target motions. *Vision Research, 23,* 1573–1583. [PubMed]

Barborica, A., & Ferrera, V. P. (2003). Estimating invisible target speed from neuronal activity in monkey frontal eye field. *Nature Neuroscience, 6,* 66–74. [PubMed]

Barborica, A., & Ferrera, V. P. (2004). Modification of saccades evoked by stimulation of frontal eye field during invisible target tracking. *Journal of Neuroscience, 24,* 3260–3267. [PubMed] [Article]

Barnes, G. R., & Asselman, P. T. (1991). The mechanism of prediction in human smooth pursuit eye movements. *The Journal of Physiology, 439,* 439–461. [PubMed] [Article]

Barnes, G. R., Barnes, D. M., & Chakraborti, S. R. (2000). Ocular pursuit responses to repeated, single-cycle sinusoids reveal behavior compatible with predictive pursuit. *Journal of Neurophysiology, 84,* 2340–2355. [PubMed] [Article]

Barnes, G. R., Donnelly, S. F., & Eason, R. D. (1987). Predictive velocity estimation in the pursuit reflex response to pseudo-random and step displacement stimuli in man. *The Journal of Physiology, 389,* 111–136. [PubMed] [Article]

Barnes, G. R., & Wells, S. G. (1999). Modelling prediction in ocular pursuit: The importance of short-term storage. In *Current oculomotor research: Physiological and psychological aspects* (pp. 97–107). New York: Plenum Press.

Becker, W., & Fuchs, A. F. (1985). Prediction in the oculomotor system: Smooth pursuit during transient disappearance of a visual target. *Experimental Brain Research, 57,* 562–575. [PubMed]

Bennett, S. J., & Barnes, G. R. (2003). Human ocular pursuit during the transient disappearance of a visual target. *Journal of Neurophysiology, 90,* 2504–2520. [PubMed] [Article]

Bennett, S. J., & Barnes, G. R. (2004). Predictive smooth ocular pursuit during the transient disappearance of a visual target. *Journal of Neurophysiology, 92,* 578–590. [PubMed] [Article]

Bennett, S. J., & Barnes, G. R. (2005). Timing the anticipatory recovery in smooth ocular pursuit during the transient disappearance of a visual target. *Experimental Brain Research, 163,* 198–203. [PubMed]

Bennett, S. J., & Barnes, G. R. (2006a). Combined smooth and saccadic ocular pursuit during the transient occlusion of a moving visual object. *Experimental Brain Research, 168,* 313–321. [PubMed]

Bennett, S. J., & Barnes, G. R. (2006b). Smooth ocular pursuit during the transient disappearance of an accelerating visual target: The role of reflexive and voluntary control. *Experimental Brain Research, 175,* 1–10. [PubMed]

Bennett, S. J., Orban de Xivry, J. J., Barnes, G. R., & Lefèvre, P. (2007). Target acceleration can be extracted and represented within the predictive drive to ocular pursuit. *Journal of Neurophysiology, 98,* 1405–1414. [PubMed] [Article]

Blohm, G., Missal, M., & Lefèvre, P. (2003). Interaction between smooth anticipation and saccades during ocular orientation in darkness. *Journal of Neurophysiology, 89,* 1423–1433. [PubMed] [Article]

Blohm, G., Missal, M., & Lefèvre, P. (2005). Direct evidence for a position input to the smooth pursuit system. *Journal of Neurophysiology, 94,* 712–721. [PubMed] [Article]

Buhusi, C. V., & Meck, W. H. (2005). What makes us tick? Functional and neural mechanisms of interval timing. *Nature Reviews, Neuroscience, 6,* 755–765. [PubMed]

Buonomano, D. V., & Karmarkar, U. R. (2002). How do we tell time? *Neuroscientist, 8,* 42–51. [PubMed]

Churchland, A. K., & Lisberger, S. G. (2002). Gain control in human smooth-pursuit eye movements. *Journal of Neurophysiology, 87,* 2936–2945. [PubMed] [Article]

Churchland, M. M., Chou, I. H., & Lisberger, S. G. (2003). Evidence for object permanence in the smooth-pursuit eye movements of monkeys. *Journal of Neurophysiology, 90,* 2205–2218. [PubMed] [Article]

Collewijn, H., van der Mark, F., & Jansen, T. C. (1975). Precise recording of human eye movements. *Vision Research, 15,* 447–450. [PubMed]

Curran-Everett, D. (2000). Multiple comparisons: Philosophies and illustrations. *American Journal of Physiology: Regulatory Integrative, and Comparative Physiology, 279,* R1–R8. [PubMed] [Article]

Dallos, P. J., & Jones, R. W. (1963). Learning behavior of the eye fixation control system. *IEEE Transactions on Automatic Control, 8,* 218–227.

de Brouwer, S., Missal, M., Barnes, G., & Lefèvre, P. (2002). Quantitative analysis of catch-up saccades during sustained pursuit. *Journal of Neurophysiology, 87,* 1772–1780. [PubMed] [Article]

de Brouwer, S., Missal, M., & Lefèvre, P. (2001). Role of retinal slip in the prediction of target motion during smooth and saccadic pursuit. *Journal of Neurophysiology, 86,* 550–558. [PubMed] [Article]

de Brouwer, S., Yuksel, D., Blohm, G., Missal, M., & Lefèvre, P. (2002). What triggers catch-up saccades during visual tracking? *Journal of Neurophysiology, 87,* 1646–1650. [PubMed] [Article]

de Hemptinne, C., Nozaradan, S., Duvivier, Q., Lefèvre, P., & Missal, M. (2007). How do primates anticipate uncertain future events? *Journal of Neuroscience, 27,* 4334–4341. [PubMed] [Article]

Ferrera, V. P., & Lisberger, S. G. (1997). Neuronal responses in visual areas MT and MST during smooth pursuit target selection. *Journal of Neurophysiology, 78,* 1433–1446. [PubMed] [Article]

Filion, C. M., Washburn, D. A., & Gulledge, J. P. (1996). Can monkeys (Macaca mulatta) represent invisible displacement? *Journal of Comparative Psychology, 110,* 386–395. [PubMed]

Heinen, S. J., Badler, J. B., & Ting, W. (2005). Timing and velocity randomization similarly affect anticipatory pursuit. *Journal of Vision, 5*(6):1, 493–503, http://journalofvision.org/5/6/1/, doi:10.1167/5.6.1. [PubMed] [Article]

Ilg, U. J., & Thier, P. (2003). Visual tracking neurons in primate area MST are activated by smooth-pursuit eye movements of an "imaginary" target. *Journal of Neurophysiology, 90,* 1489–1502. [PubMed] [Article]

Kettner, R. E., Mahamud, S., Leung, H. C., Sitkoff, N., Houk, J. C., Peterson, B. W., et al. (1997). Prediction of complex two-dimensional trajectories by a cerebellar model of smooth pursuit eye movement. *Journal of Neurophysiology, 77,* 2115–2130. [PubMed] [Article]

Madelain, L., & Krauzlis, R. J. (2003). Effects of learning on smooth pursuit during transient disappearance of a visual target. *Journal of Neurophysiology, 90,* 972–982. [PubMed] [Article]

Martinez-Trujillo, J. C., & Treue, S. (2004). Feature-based attention increases the selectivity of population responses in primate visual cortex. *Current Biology, 14,* 744–751. [PubMed] [Article]

Mitrani, L., & Dimitrov, G. (1978). Pursuit eye movements of a disappearing moving target. *Vision Research, 18,* 537–539. [PubMed]

Mrotek, L. A., & Soechting, J. F. (2007). Predicting curvilinear target motion through an occlusion. *Experimental Brain Research, 178,* 99–114. [PubMed]

Orban de Xivry, J. J., Bennett, S. J., Lefèvre, P., & Barnes, G. R. (2006). Evidence for synergy between saccades and smooth pursuit during transient target disappearance. *Journal of Neurophysiology, 95,* 418–427. [PubMed] [Article]

Orban de Xivry, J. J., & Lefèvre, P. (2007). Saccades and pursuit: Two outcomes of a single sensorimotor process. *The Journal of Physiology, 584,* 11–23. [PubMed] [Article]

Pola, J., & Wyatt, H. J. (1997). Offset dynamics of human smooth pursuit eye movements: Effects of target presence and subject attention. *Vision Research, 37,* 2579–2595. [PubMed]

Robinson, D. A. (1963). A method of measuring eye movement using a scleral search coil in a magnetic field. *IEEE Transactions on Biomedical Engineering, 10,* 137–145. [PubMed]

Shibata, T., Tabata, H., Schaal, S., & Kawato, M. (2005). A model of smooth pursuit in primates based on learning the target dynamics. *Neural Networks, 18,* 213–224. [PubMed]

Tanaka, M., & Lisberger, S. G. (2001). Regulation of the gain of visually guided smooth-pursuit eye movements by frontal cortex. *Nature, 409,* 191–194. [PubMed]

Treue, S., & Martinez Trujillo, J. C. (1999). Feature-based attention influences motion processing gain in macaque visual cortex. *Nature, 399,* 575–579. [PubMed]

Whittaker, S. G., & Eaholtz, G. (1982). Learning patterns of eye motion for foveal pursuit. *Investigative Ophthalmology & Visual Science, 23,* 393–397. [PubMed] [Article]

Xiao, Q., Barborica, A., & Ferrera, V. P. (2007). Modulation of visual responses in macaque frontal eye field during covert tracking of invisible targets. *Cerebral Cortex, 17,* 918–928. [PubMed] [Article]